Journal of Biomedical Optics

BiomedicalOptics.SPIEDigitalLibrary.org

Combination of low level light therapy and nitrosyl-cobinamide accelerates wound healing

Ryan Spitler
Hsiang Ho
Frederique Norpetlian
Xiangduo Kong
Jingjing Jiang
Kyoko Yokomori
Bogi Andersen
Gerry R. Boss
Michael W. Berns

SPIE.

Journal of Biomedical Optics 20(5), 051022 (May 2015)

Combination of low level light therapy and nitrosyl-cobinamide accelerates wound healing

Ryan Spitler,[a,*] Hsiang Ho,[a] Frederique Norpetlian,[a] Xiangduo Kong,[a] Jingjing Jiang,[b] Kyoko Yokomori,[a] Bogi Andersen,[a] Gerry R. Boss,[b] and Michael W. Berns[a,b]
[a]University of California Irvine, Irvine, California 92612 United States
[b]University of California San Diego, La Jolla, California 92093 United States

Abstract. Low level light therapy (LLLT) has numerous therapeutic benefits, including improving wound healing, but the precise mechanisms involved are not well established; in particular, the underlying role of cytochrome C oxidase (C-ox) as the primary photoacceptor and the associated biochemical mechanisms still require further investigation. We previously showed the nitric oxide (NO) donating drug nitrosyl-cobinamide (NO-Cbi) enhances wound healing through a cGMP/cGMP-dependent protein kinase/ERK1/2 mechanism. Here, we show that the combination of LLLT and NO-Cbi markedly improves wound healing compared to either treatment alone. LLLT-enhanced wound healing proceeded through an electron transport chain-C-ox-dependent mechanism with a reduction of reactive oxygen species and increased adenosine triphosphate production. C-ox was validated as the primary photoacceptor by three observations: increased oxygen consumption, reduced wound healing in the presence of sodium azide, and disassociation of cyanide, a known C-ox ligand, following LLLT. We conclude that LLLT and NO-Cbi accelerate wound healing through two independent mechanisms, the electron transport chain-C-ox pathway and cGMP signaling, respectively, with both resulting in ERK1/2 activation. [DOI: 10.1117/1.JBO.20.5.051022]

Keywords: laser; light-emitting diode; wound healing; cell migration; low level light therapy.

Paper 140423SSRR received Jul. 1, 2014; accepted for publication Dec. 4, 2014; published online Jan. 6, 2015.

1 Introduction

Low level light therapy (LLLT) is a promising modality for a variety of medical conditions, but the underlying mechanisms of LLLT warrant further investigation.[1–3] An important aspect of the mechanism is validating the photoacceptor molecule, because an absorbing molecule is necessary for light energy to be converted into chemical energy that can be used by cells.[4] The biomodulation of cellular activities has been shown to be wavelength dependent demonstrating no effect from white light at similar optical parameters to the study presented.[5] The multimolecular complexes of the electron transport system have been suggested as the light receptors, and that light increases metabolic activity.[6] LLLT increases mitochondrial activity of complexes I, II, III, IV, and succinate dehydrogenase,[7] with cytochrome C oxidase (C-ox), part of complex IV, generally accepted as the primary photoaccepting molecule. Evidence for a C-ox-dependent LLLT mechanism includes increased oxygen consumption during LLLT—the majority of total cellular oxygen consumption occurs at complex IV,[6,8] and the absorption spectrum of C-ox intermediates is similar to the known action spectra of LLLT.[4] Changes in reactive oxygen species (ROS)[9–11] have also been reported, as well as increases in adenosine triphosphate (ATP) production.[12–17] Increased cellular nitric oxide (NO) also occurs from either NO release from metal complexes[11] or up-regulation of the expression of inducible NO synthase (iNOS).[18]

We now further validate C-ox as the primary photoacceptor because: (1) LLLT increases cellular oxygen consumption, (2) C-ox inhibition reverses wound healing induced by LLLT, and (3) LLLT decreases the intracellular concentration of cyanide, a known ligand of C-ox. Other observations include a reduction of cellular ROS and an increase in ATP production, which implies more efficient electron flow through the electron transport chain.

In separate work, we demonstrated that LLLT and nitrosyl-cobinamide (NO-Cbi) increased wound healing.[19,20] Here, we demonstrate that the combination of LLLT and NO-Cbi produces much greater wound healing than either treatment alone. In addition, we show that the functional response of each modality proceeds through a different biochemical pathway: the electron transport chain and cGMP, respectively, with both resulting in ERK1/2 (extracellular signal-regulated kinase) activation.

2 Material and Methods

2.1 *Cell Culture*

U2OS human osteosarcoma cells were obtained from the American Type Tissue Culture Collection (ATCC, Rockville, Maryland). Cells were grown in T-75 flasks (Corning, Fisher, Pittsburgh, Pennsylvania) in a 37°C, 5% CO_2/95% air incubator using Dulbecco's modified Eagle's medium and supplemented with 10% fetal bovine serum (Mediatach, Manassas, Virginia). Cells were trypsinized with TrypLE (Invitrogen Life Technologies, Carlsbad, California), seeded into 6-well or 96-well plates (Corning, Fisher) and grown to confluence.

*Address all correspondence to: Ryan Spitler, E-mail: rspitler@stanford.edu

0091-3286/2015/$25.00 © 2015 SPIE

2.2 *Light Irradiation Devices*

The light sources and parameters of delivery were previously described.[20] Briefly two light sources were used, a laser (Biolitec AG, Jena, Germany) and a light-emitting diode (LED) array (Biophotas Inc., Tustin, California) with the following parameters: Laser 652 and 806 nm with a full bandwidth of 5 nm; LED 637 and 901 nm with full bandwidths of 17 and 69 nm, respectively. The duration of treatment time for both sources was 1800 s with a power density of 5.57 and 1.30 mW/cm^2 for the red and near infrared ranges, respectively, and with corresponding energy densities of 10.02 and 2.334. The spot diameter from the laser source was 12.5 cm. The laser and LED power were measured with a FieldMate laser power meter (Coherent, Santa Clara, California). All samples were kept under low level light or in the dark before and after irradiation.

2.3 *Heat Measurements*

Cell culture temperature was measured using a RAYNGER MX4 (Raytek, Santa Cruz, California) infrared-detecting thermometer/laser temperature gun as previously described.[20] A fan was used to eliminate heat transfer from the LED circuitry. The cell culture temperature was measured before and after treatment.

2.4 *Pharmacological Treatments*

Cells were treated with the following compounds: 50-μM sodium azide, 100-μM sodium cyanide (Sigma-Aldrich, St. Louis, Missouri), 5-μM U1026 (Promega, Madison, Wisconsin) and 5-μM NO-Cbi.

2.5 *Combined Pharmacological and Light Treatment*

Cells were exposed to LLLT for 30 min and 1 h later received a single treatment of 5-μM NO-Cbi.

2.6 *Preparation of NO-Cbi*

Cobinamide was produced by base hydrolysis of hydroxocobalamin (Sigma-Aldrich) as described previously.[21] The cobalt was reduced from a +3 to +2 valency state using a two-molar excess of ascorbic acid in a deoxygenated solution. NO gas (99.99% pure, Matheson Gas Co.) was bubbled through the reduced cobinamide solution, and excess NO was removed by bubbling argon through the solution.[22] Concentrated stock solutions of NO-Cbi were diluted in deoxygenated sterile water, and the diluted NO-Cbi was added to the cells using a Hamilton syringe (Hamilton, Reno, Nevada).

2.7 *Scratch Wound Closure Assay*

The scratch wound closure assay has been previously described.[19] Briefly 600 to 700-μm-wide single-line scratches were mechanically generated in a cell monolayer by a 200-μl plastic tip (~450 to 600 μm at the tip) across the length of the well. Multiple images were acquired along the length of the scratch to ensure representative sampling areas for each gap. Cells from both edges of the wound migrated into the open area, which was measured at 24 h. The change in area was quantified using a custom MATLAB script, which blurred the image and subtracted the blurred image from the original image. Smooth regions (the scratch wound) have less of a difference between the blurred and original images, thus generating a clear wound boundary. Once the boundary was determined pseudocolor was added by the custom script, which mapped the gap of the scratch wound. Images with similar intensities can be quantified using the same threshold and blur-block parameters; however, these may be adjusted for images with varying intensities. This method allowed for very accurate measurement of wound areas. The wound closure rate was determined by plotting changes in the wound area as a function of time.

2.8 *MTS Cell Proliferation*

U2OS cells were seeded at 2×10^4 per well in a 96-well plate format and incubated overnight to permit cell attachment. At 24-h post-treatment (LLLT ± NO-Cbi) cell proliferation was determined using an MTS [3(4,5-dimethylthiazol-2-yl)-5-(3-car-boxymethoxyphenyl)-2-(4-sulfophenyl)-2*H*-tetrazolium] proliferation assay (CellTiter 96® AQueous Non-Radioactive Cell Proliferation Assay; Promega, Madison, Wisconsin) according to the manufacturer's instructions. The MTS dye was added directly to the cell culture media and incubated with the cells for 2 h at 37°C. The dye absorbance at 490 nm was measured and plotted for all treatment conditions.

2.9 *Microscopy*

Phase contrast images were captured through a 10× magnification Ph1 na (numerical aperture) 0.25 objective (Zeiss, Jena, Germany). An inverted microscope (Axiovert 135, Zeiss) with a charge-coupled device (CCD) camera (ORCA-R^2 Hamamatsu, Bridgewater, New Jersey) was used. Images were acquired using custom Robolase II software.[23]

2.10 *Cellular ROS Detection*

About 2.0×10^4 cells were seeded into each well of a black 96-well plate and allowed to attach overnight. Cells were loaded with 25-μM cell permeant reagent (2',7'-dichlorofluorescein diacetate, DCFDA, Abcam, Cambridge, Massachusetts) for 45 min. This compound detects hydrogen peroxide, superoxide, and other ROS species.[24] Cells were then washed and treated with LLLT. ROS levels were measured immediately after LLLT treatment and detected using a plate reader with a 485-nm excitation and 535-nm emission filter set.

2.11 *ATP Measurement*

Cells treated as described above were exposed to LLLT. Cells were extracted immediately after LLLT treatment, and the ATP concentration in the extracts was measured according to manufacturer's instructions using the ATPLite kit (PerkinElmer Life Sciences, Boston, Massachusetts).

2.12 *Oxygen Consumption*

A total of 1.0×10^6 intact live cells were loaded into the chamber of an Oxytherm System type Clark electrode (Hansatech Instruments, Pentney, England) as a suspension after trypsinzation. Oxygen consumption rates were allowed to stabilize for 5 min prior to data acquisition by Oxygraph Plus software (Hansatech Instruments, Pentney, England). LLLT was applied to the sample while in the chamber. No respiratory substrates were added to the sample mixture as oxygen levels were

measured from live cells. Oxygen consumption was measured in live cells in real time for 5 min. The rate of oxygen consumption was determined using the software curve fitting function.

2.13 *Cyanide Analysis*

A concentration of 100-μM NaCN dissolved in 0.1-M NaOH was administered to cell cultures in a confluent 6-well dish followed by either immediate LLLT, or no treatment. After 30 min, the culture media was harvested by aspiration, and the cells were washed three times in PBS before being extracted in situ using 1 ml of RIPA Lysis and Extraction buffer (Thermo Scientific, Rockford, Illinois). A volume of 500 μl of cell extract or media was added to the outer well of a Conway microdiffusion cell and 500 μl of 10% trichloroacetic acid (TCA) was added to the opposite side of the same well to prevent premature mixing. Next a volume of 250 μl of ice-cold 30-μM cobinamide (Cbi) in 0.1-M NaOH was added to the inner well.[21] Once the cells were capped, the TCA was mixed with the sample to convert CN^- to HCN, which is volatile. The Conway cells were incubated for 25 min at room temperature to allow for the cyanide to diffuse to the center well and bind to Cbi. The solution in the center well was collected, and absorbance at 366 nm was measured using a spectrophotometer. Cyanide concentrations of the samples were determined from a standard curve.

2.14 *Western Blots*

Cells were serum starved overnight, lysed and harvested 8 min after treatment in Laemmli buffer heated to 100°C (BioRad, Hercules, California), and lysates were sonicated and resolved on SDS-PAGE gels. The proteins were transferred to a nitrocellulose membrane (GE Healthcare Life Sciences, Pittsburgh) and blocked for 1 h with Pierce Protein-Free Blocking buffer (Thermo Scientific). They were incubated overnight with antibodies for phospho-ERK1/2(Thr202/Tyr203) and total ERK1/2 at 1:10,000 in TBS/5% BSA (Cell Signaling Technology). Membranes were then incubated with an anti-rabbit-HRP antibody at 1 : 2000 for 1 h and developed using a luminol-based chemiluminescent substrate. pERK1/2 and ERK intensity for each condition was quantified separately using ImageJ[25] and then normalized respectively to total ERK1/2 and the untreated control.

2.15 *Statistical Analysis*

Data are presented as mean ± standard error of the mean (SEM). Student's *t*-tests were used for experiments that contained only two variables, and one-way analysis of variance followed by Bonferroni's post-test was used for experiments containing three or more variables. A P value <0.05 was considered statistically significant. All experiments have been repeated at least three times with the technical replicate number indicated for each dataset. The presented data are an average of all replicates resulting from at least three separate experiments.

3 Results

3.1 *Combination of NO-Cbi and LLLT Induces Wound Healing Much More Effectively Than Either Treatment Alone*

As we showed previously, NO-Cbi and LLLT enhance wound healing in cellular models [Figs. 1(a) and 1(b)].[19,20] We now show that combining NO-Cbi and LLLT markedly enhanced wound healing compared to either treatment alone [Figs. 1(a) and 1(b)]. This effect was observed for all LLLT wavelengths tested and for light delivered by a laser or LEDs. No statistically significant difference in cell proliferation was observed for all conditions tested compared to the untreated control [Fig. 1(c)].

3.2 *C-ox and Electron Transport are Required for LLLT to Enhance Wound Healing*

We performed several sets of experiments to determine if the effects of LLLT were mediated through the electron transport system and a C-ox-dependent mechanism. First, we found that sodium azide, a C-ox inhibitor, abolished LLLT-enhanced wound healing [Figs. 2(a) and 2(b)]. Second, we observed increased oxygen consumption occurred almost immediately following LLLT (Table 1). Third, LLLT decreased ROS and increased ATP concentrations in U2OS cells [Figs. 3(a) and 3(b)], indicating increased electron flow through the electron transport chain. And fourth, we took advantage of the tight binding of cyanide to C-ox, and treated cells with nontoxic concentrations of cyanide, i.e., cyanide concentrations that did not reduce rates of wound healing, and then measured the intracellular cyanide concentration. We found that the cyanide concentration was significantly lower in extracts of LLLT-treated cells than in control cells (Table 2). These data suggest that cyanide bound to C-ox within the cell was released when the cells were exposed to LLLT, and that the cyanide diffused into the culture media. The predicted increase in the cyanide concentration in the media was extremely small (~5 pmol), which is below the detection limit of the assay, and, indeed, we found no change in the media cyanide concentration (Table 2). We provide a more in-depth explanation of this observation in the discussion section.

3.3 *NO-Cbi-Induced and LLLT Induce ERK Activation*

As shown previously, we found that NO-Cbi increased ERK1/2 activation [Fig. 4(a)]. LLLT also increased ERK1/2 activation at all wavelengths tested [Fig. 4(a)]. The combination of NO-Cbi and LLLT yielded varying degrees of ERK1/2 activation compared to individual treatments; however, differences between conditions were minimal. The scratch migration assay was conducted in combination with specific inhibitors for mitogen-activated protein kinase/extracellular-signal-regulated kinase (MEK/ERK) and C-ox using U0126 and sodium azide respectively [Fig. 4(b)]. The laser 652-nm wavelength was selected to investigate the interplay between light and NO-Cbi, because strong activation of the ERK1/2 pathway was observed. The U0126 inhibitor prevented both the NO-Cbi and laser 652-nm enhancement of wound healing. Sodium azide only prevented laser 652 nm while having no effect on NO-Cbi. The beneficial effect from the combined treatment of NO-Cbi and laser 652 nm was decreased when either inhibitor was used. When added alone, neither U0126 or sodium azide, had an effect on wound healing in the absence of NO-Cbi, laser 652 nm or both combined. These data indicate that both individual and combined treatments of NO-Cbi and laser 652 nm require MEK/ERK1/2.

4 Discussion

We identified four wavelengths of light that improved wound healing in U2OS cells and found that the combination of light and an NO donor strikingly accelerates wound healing.

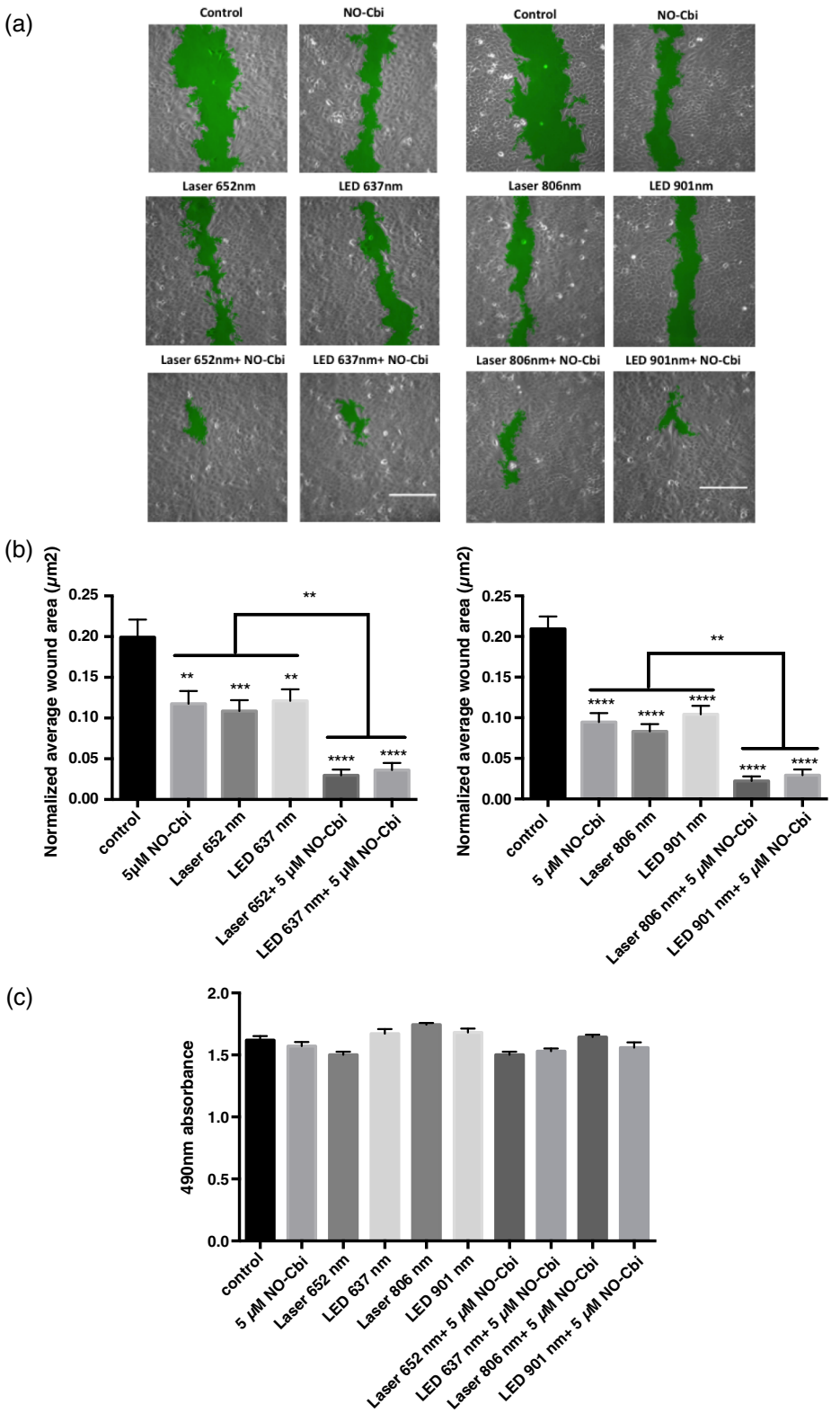

Fig. 1 Wound healing induced by low level light therapy (LLLT) and NO-Cbi. (a and b) U2OS cells received a mechanical scratch wound followed by treatment with LLLT, 5 μM NO-Cbi, or the combination of LLLT and NO-Cbi. Wound recovery was followed for a period of 24 h at which time the final wound area was determined and normalized to the initial wound size. The images being shown are at 24-h post-treatment. The normalized average wound area was determined by dividing the final wound area by the initial quantified wound area and averaging the replicates. The green area marks the wound. Bar, 100 μm. (c) The MTS proliferation assay showed no statistically significant differences between the untreated control. Data represent the mean $\pm$ standard error of the mean (SEM) of at least three separate experiments with $n = 12$ (a and b) or $n = 6$ for (c) per experiment. $^{****}P < 0.0001$, $^{***}P < 0.001$, and $^{**}P < 0.01$ compared to untreated control or indicated comparison.

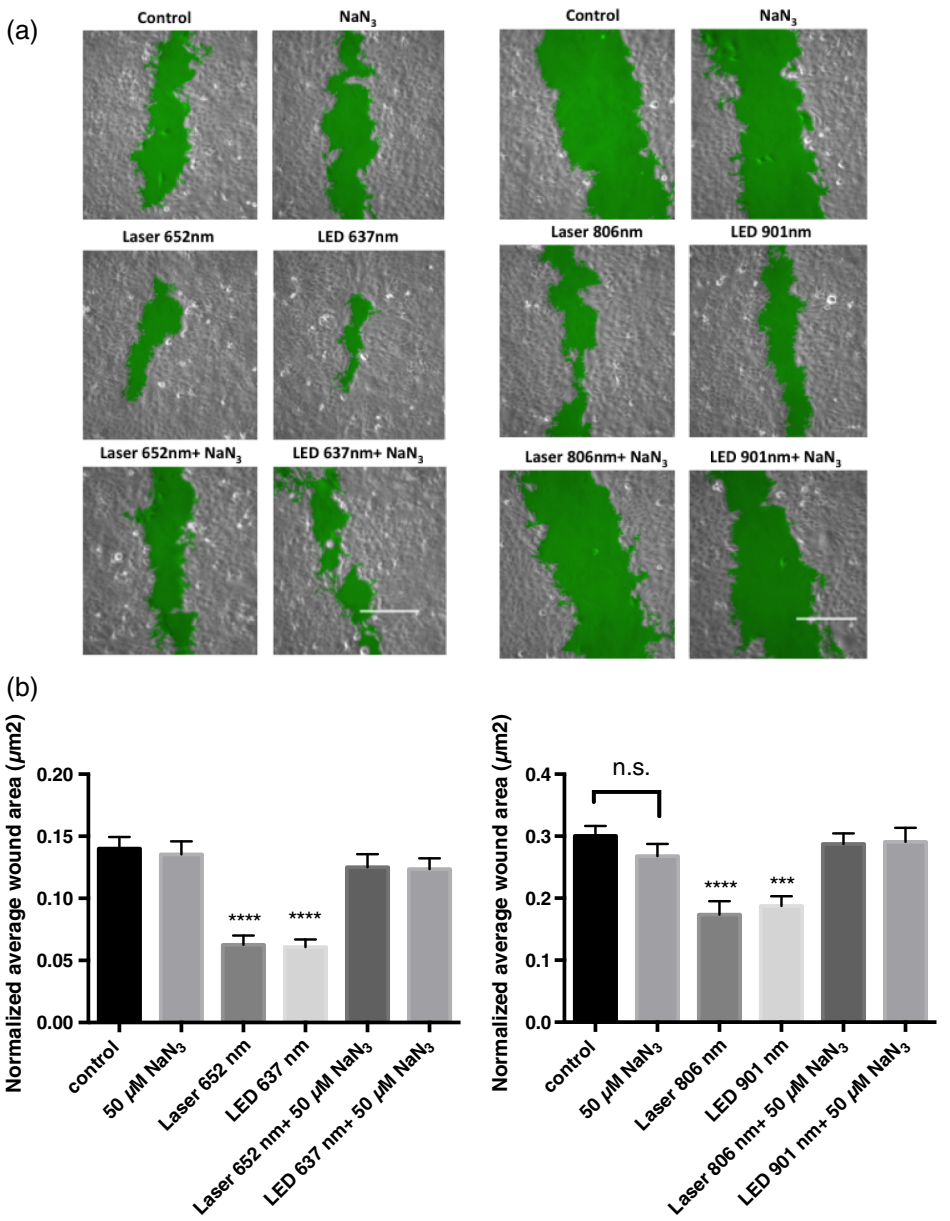

Fig. 2 Sodium azide inhibits wound healing after LLLT Treatment. (a and b). A mechanical scratch wound was generated in U2OS cells, and the cells were treated with 50-μM sodium azide, a cytochrome C oxidase inhibitor. The wound closure rate was quantified after 24 h. The images being shown are at 24-h post-treatment. The green area marks the wound. Bar, 100 μm. Data represent the mean $\pm$ SEM of at least three separate experiments with $n = 12$ per experiment. ****$P < 0.0001$ and ***$P < 0.001$ compared to untreated control.

Consistent with our previous findings, the combined treatment appears to accelerate wound healing primarily through cell migration and to a lesser extent through cell proliferation. LLLT decreased cellular ROS concentrations and increased cellular ATP, suggesting increased electron flow through the electron transport chain following light treatment. Although a number of studies report an increase of cellular ROS resulting in activation of redox sensitive transcription factors, we observed a decrease in ROS.[26–28] There are at least two possible explanations for this difference in results: (1) LLLT triggered only a transient increase of ROS, which was no longer detectable after the 30-min treatment period used in our assay, or (2) LLLT triggered the up regulation of superoxide dismutase or catalase, which would significantly reduce cellular ROS.

Our data suggest that C-ox is the primary photoacceptor for several reasons: (1) sodium azide, a C-ox inhibitor, prevented the beneficial effect of LLLT; (2) LLLT increased oxygen consumption, and C-ox accounts for the majority of oxygen consumption within the cell; and (3) LLLT reduced intracellular cyanide, likely by releasing it from C-ox, the main cellular cyanide-binding protein. We conclude that LLLT proceeds mainly through an electron transport chain-C-ox-dependent mechanism. However, this does not exclude the possibility that other cellular chromophores absorb light and convert it to chemical energy. It is also possible that some of the oxygen consumption could be due to mitochondria uncoupling; however, we do not believe this to be the case.

Although the cyanide concentration decreased in the cell extract, no measurable change in cyanide was detected in the

Table 1 Low level light therapy (LLLT) increases oxygen consumption rates. Oxygen consumption rates were measured in intact U2OS cells for 5 min, and then for an additional 5 min immediately following LLLT treatment. Data represent the mean ± SEM of at least three separate experiments with $n = 3$ per experiment. ****$P < 0.0001$ compared to untreated control.

Treatment condition	Oxygen consumption rate (nmol/1×10^6 cells/min)
Control	0.79 ± 0.03
Laser 652 nm	3.71 ± 0.13****
Laser 806 nm	3.42 ± 0.14****
LED 637 nm	3.46 ± 0.20****
LED 901 nm	4.30 ± 0.22****

Table 2 LLLT causes cyanide disassociation from C-ox. U2OS cells were treated with 100-μM sodium cyanide, and then some cells were immediately exposed to LLLT for 30 min. Media and cell extract samples were harvested and cyanide concentration was determined. Data represent the mean ± SEM of at least three separate experiments with $n = 2$ per experiment. **$P < 0.01$ compared to untreated control.

Treatment condition	Media cyanide concentration (μM)	Cellular cyanide concentration (μM)
Control	5.82 ± 0.10	4.38 ± 0.40
Laser 652 nm	5.82 ± 0.12	3.04 ± 0.12**
Laser 806 nm	5.84 ± 0.37	3.05 ± 0.29**
LED 637 nm	5.80 ± 0.14	2.88 ± 0.22**
LED 901 nm	5.79 ± 0.21	2.39 ± 0.06**

media. This likely can be explained as follows: a total of 1.2×10^6 cells were present in one well of a confluent cell monolayer in 1 ml of culture medium. The volume of one U2OS cell is ~4 pL,[29] yielding a total cell volume of 4.8 μl per well. Thus, only ~5 pmol could diffuse into the cell media, which is below the detection limit of the assay.

We showed previously that the NO-Cbi improves wound healing through a cGMP/cGMP-dependent protein kinase/ERK1/2 pathway, and we now show that the NO-Cbi-induced ERK1/2 activation also occurs in the presence of light. We conclude that NO-Cbi and LLLT improve wound healing through cGMP and the electron transport chain-C-ox pathway, both resulting in ERK1/2 activation. The differences observed in ERK1/2 activation may be explained by the cell types' responsiveness to the optical parameters used, however, the differences are minimal. Furthermore, we have demonstrated that ERK1/2 activation occurs for all conditions tested and appears to be required for increased wound closure. Not all wavelengths were investigated using specific inhibitors; however, laser 652 nm was investigated and found to require MEK/ERK for both combination treatment with NO-Cbi and alone.

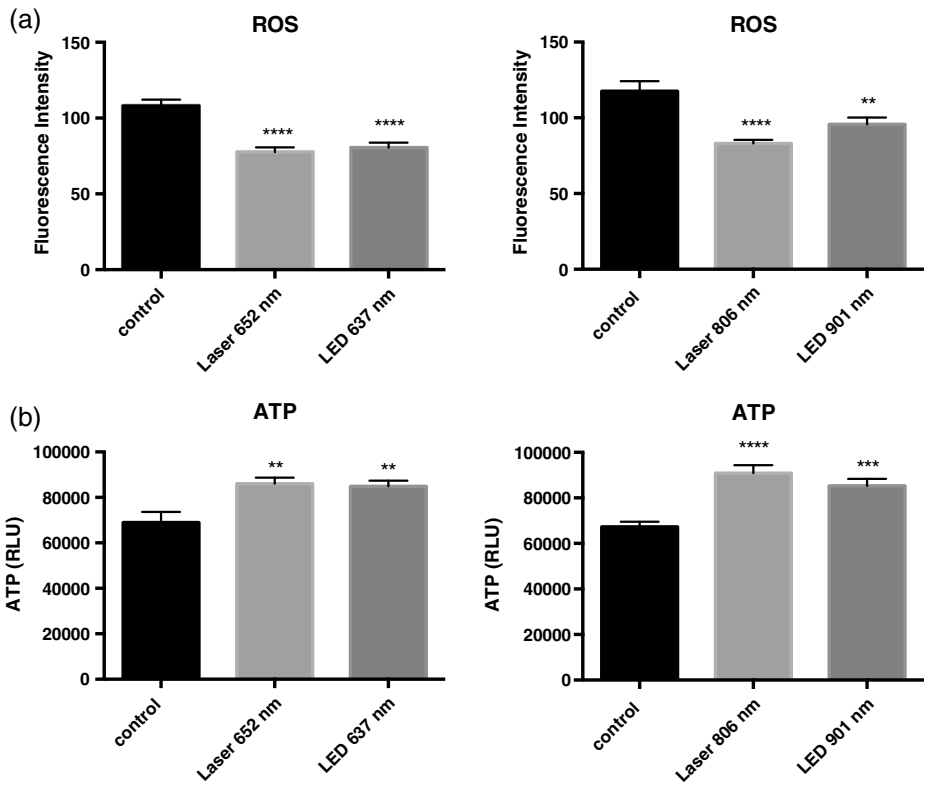

Fig. 3 LLLT reduces reactive oxygen species (ROS) and increases ATP concentrations. (a) U2OS cells were incubated with DCFDA dye and cellular ROS was measured as described in Sec. 2. (b) A cell extract was prepared immediately following LLLT treatment and ATP was measured using a luciferase-based assay. Data represent the mean ± SEM of at least three separate experiments with $n = 4$ per experiment. ****$P < 0.0001$, ***$P < 0.001$, and **$P < 0.01$ compared to untreated control.

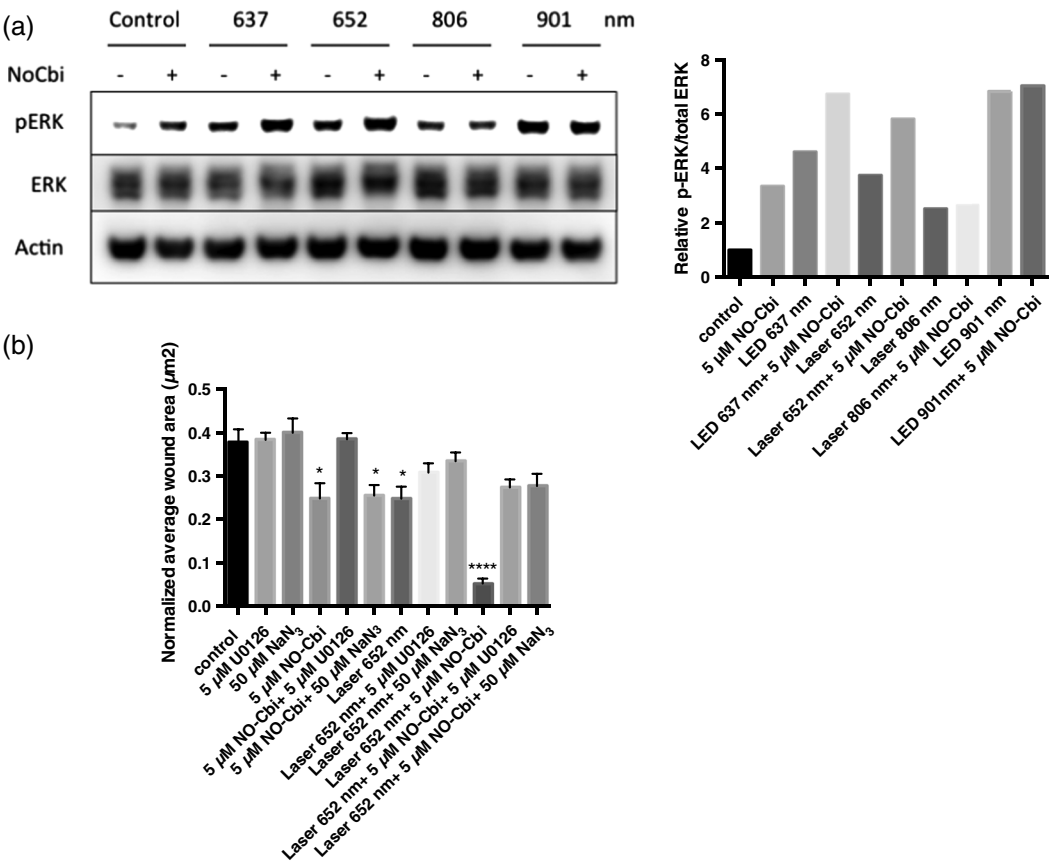

Fig. 4 Western blot and migration analysis of phospho-ERK1/2. (a) U2OS cells were treated with NO-Cbi, LLLT, or a combination of LLLT and NO-Cbi. ERK1/2 phosphorylation and total ERK1/2 expression were determined by western blot analysis (left). The intensity of pERK1/2 expression was quantified and then normalized to the total ERK1/2 expression and the untreated control (right). (b) A mechanical scratch wound was generated in U2OS cells, and the cells were treated with 50-μM sodium azide, a C-ox inhibitor and 5-μM U0126, an MEK-specific inhibitor. The wound closure rate was quantified after 24 h. Data are representative of at least three separate experiments for (a) and data represent the mean $\pm$ SEM of at least three separate experiments with $n = 12$ per experiment for (b). $^{****}P < 0.0001$ and $^{*}P < 0.05$ compared to untreated control.

Low levels of nitric oxide have been associated with beneficial effects whether occurring through release from C-ox or from increased NOS activity as a result of LLLT.[30] These findings seem to suggest that C-ox can still function normally when low concentrations of nitric oxide are present. In the current study, cells were first treated with LLLT, given 1 h to allow for downstream effects to occur and then given a low dose of nitric oxide (5 μM) delivered by NO-Cbi. We think that this delay and separation of individual treatments is what allows for the observed synergistic wound healing effect. Since nitric oxide is a known inhibitor of C-ox, adding NO-Cbi too close to the LLLT treatment will inhibit the enhanced effect observed from the combined treatment.

We do not exclude the possibility that NO-Cbi and LLLT may stimulate additional pathways. Although this work was conducted *in vitro*, it does suggest a potential clinical application for wound healing and other areas where a low level light is used as a biostimulation agent.

Acknowledgments

This work was supported by the Military Photomedicine Program, AFOSR Grant# FA9550-08-1-0384, Biophotas, Inc. Research Fellowship, the CounterACT Program, Office of the Director, National Institutes of Health, National Institute of Neurological Diseases and Stroke, U01 NS058030 and NIAMS, 1 F32 AR065356-01A1 National Institutes of Health. We would also like to acknowledge Eric Cam from the Andersen lab for assistance with western blots.

References

1. W. Posten et al., "Low-level laser therapy for wound healing: mechanism and efficacy," *Dermatol. Surg.* **31**(3), 334–340 (2005).
2. H. Chung et al., "The nuts and bolts of low-level laser (light) therapy," *Ann. Biomed. Eng.* **40**(2), 516–533 (2012).
3. N. J. Prindeze, L. T. Moffatt, and J. W. Shupp, "Mechanisms of action for light therapy: a review of molecular interactions," *Exp. Biol. Med.* **237**(11), 1241–1248 (2012).
4. T. I. Karu and S. F. Kolyakov, "Exact action spectra for cellular responses relevant to phototherapy," *Photomed. Laser Surg.* **23**(4), 355–361 (2005).
5. R. Sroka et al., "Effects on the mitosis of normal and tumor cells induced by light treatment of different wavelengths," *Lasers Surg. Med.* **25**(3), 263–271 (1999).
6. W. Yu et al., "Photomodulation of oxidative metabolism and electron chain enzymes in rat liver mitochondria," *Photochem. Photobiol.* **66**(6), 866–871 (1997).
7. P. C. Silveira et al., "Evaluation of mitochondrial respiratory chain activity in muscle healing by low-level laser therapy," *J. Photochem. Photobiol. B* **95**(2), 89–92 (2009).

8. D. Pastore et al., "Increase in <–H+/e- ratio of the cytochrome c oxidase reaction in mitochondria irradiated with helium-neon laser," *Biochem. Mol. Biol. Int.* **34**(4), 817–826 (1994).
9. A. C. Chen et al., "Low-level laser therapy activates NF-kB via generation of reactive oxygen species in mouse embryonic fibroblasts," *PLoS One* **6**(7), e22453 (2011).
10. Y. Y. Huang et al., "Low-level laser therapy (LLLT) reduces oxidative stress in primary cortical neurons in vitro," *J. Biophotonics* **6**(10), 829–838 (2013).
11. A. Lindgard et al., "Irradiation at 634 nm releases nitric oxide from human monocytes," *Lasers Med. Sci.* **22**(1), 30–36 (2007).
12. U. Oron et al., "Ga-As (808 nm) laser irradiation enhances ATP production in human neuronal cells in culture," *Photomed. Laser Surg.* **25**(3), 180–182 (2007).
13. S. Passarella et al., "Increase of proton electrochemical potential and ATP synthesis in rat liver mitochondria irradiated in vitro by helium-neon laser," *FEBS Lett.* **175**(1), 95–99 (1984).
14. T. Karu, L. Pyatibrat, and G. Kalendo, "Irradiation with He-Ne laser increases ATP level in cells cultivated in vitro," *J. Photochem. Photobiol. B* **27**(3), 219–223 (1995).
15. M. J. Conlan, J. W. Rapley, and C. M. Cobb, "Biostimulation of wound healing by low-energy laser irradiation. A review," *J. Clin. Periodontol.* **23**(5), 492–496 (1996).
16. T. Karu, "Primary and secondary mechanisms of action of visible to near-IR radiation on cells," *J. Photochem. Photobiol. B* **49**(1), 1–17 (1999).
17. L. Wilden and R. Karthein, "Import of radiation phenomena of electrons and therapeutic low-level laser in regard to the mitochondrial energy transfer," *J. Clin. Laser Med. Surg.* **16**(3), 159–165 (1998).
18. R. Zhang et al., "Near infrared light protects cardiomyocytes from hypoxia and reoxygenation injury by a nitric oxide dependent mechanism," *J. Mol. Cell Cardiol.* **46**(1), 4–14 (2009).
19. R. Spitler et al., "Nitrosyl-cobinamide (NO-Cbi), a new nitric oxide donor, improves wound healing through cGMP/cGMP-dependent protein kinase," *Cell Signal* **25**(12), 2374–2382 (2013).
20. R. Spitler and M. W. Berns, "Comparison of laser and diode sources for acceleration of in vitro wound healing by low-level light therapy," *J. Biomed. Opt.* **19**(3), 038001 (2014).
21. W. C. Blackledge et al., "New facile method to measure cyanide in blood," *Anal. Chem.* **82**(10), 4216–4221 (2010).
22. K. E. Broderick et al., "Nitrosyl-cobinamide, a new and direct nitric oxide releasing drug effective in vivo," *Exp. Biol. Med.* **232**(11), 1432–1440 (2007).
23. E. L. Botvinick and M. W. Berns, "Internet-based robotic laser scissors and tweezers microscopy," *Microsc. Res. Tech.* **68**(2), 65–74 (2005).
24. S. L. Hempel et al., "Dihydrofluorescein diacetate is superior for detecting intracellular oxidants: comparison with 2',7'-dichlorodihydrofluorescein diacetate, 5(and 6)-carboxy-2',7'-dichlorodihydrofluorescein diacetate, and dihydrorhodamine 123," *Free Radical Biol. Med.* **27**(1–2), 146–159 (1999).
25. C. A. Schneider, W. S. Rasband, and K. W. Eliceiri, "NIH Image to ImageJ: 25 years of image analysis," *Nat. Methods* **9**(7), 671–675 (2012).
26. N. Grossman et al., "780 nm low power diode laser irradiation stimulates proliferation of keratinocyte cultures: involvement of reactive oxygen species," *Lasers Surg. Med.* **22**(4), 212–218 (1998).
27. R. Lavi et al., "Detailed analysis of reactive oxygen species induced by visible light in various cell types," *Lasers Surg. Med.* **42**(6), 473–480 (2010).
28. R. Lubart et al., "Low-energy laser irradiation promotes cellular redox activity," *Photomed. Laser Surg.* **23**(1), 3–9 (2005).
29. M. Beck et al., "The quantitative proteome of a human cell line," *Mol. Syst. Biol.* **7**, 549 (2011).
30. R. O. Poyton and K. A. Ball, "Therapeutic photobiomodulation: nitric oxide and a novel function of mitochondrial cytochrome c oxidase," *Discov. Med.* **11**(57), 154–159 (2011).

Ryan Spitler is a postdoctoral research fellow at Stanford University. He completed his PhD degree at the University of California, Irvine, working in the Beckman Laser Institute and his BS degree from the University of California, Santa Cruz. He is also the recipient of the Biophotas Fellowship to investigate the cellular response to LED therapy in the context of wound healing.

Michael W. Berns is a professor of biomedical engineering, surgery and cell biology at the University of California, Irvine, and adjunct professor in the Department of Bioengineering at the University of California, San Diego. He received BS, MS, and PhD degrees from Cornell University, New York. He is the cofounder of the Beckman Laser Institute and Medical Clinic with philanthropist Arnold O. Beckman and chairman and CEO of the nonprofit Beckman Laser Institute Inc.

Biographies of the other authors are not available.